Marine Vehicle Spectrum Signature Detection Based On An Adaptive CFAR and Multi-Frame Fusion Algorithms

Dahai Cheng *ericdahaicheng@qq.com*
School of Electric and Automatic Engineering
Changshu Institute of Technology
Changshu, Jiangsu, China. 215500

Abstract

Detecting marine vehicle spectrum signature from hydrophone at low false alarm rate and high detection rate in an environment of various interference is a very difficult problem. To overcome this problem, an observation space is created by sampling and dividing input analog acoustic signal into digital signal in multiple frames and each frame is transformed into the frequency domain; then an Adaptive Constant False Alarm Rate (ACFAR) and Post Detection Fusion algorithms have been proposed for an effective automatic detection of marine vehicle generated acoustic signal spectrum signature. The proposed algorithms have been tested on several real acoustic signals. The statistical analysis and experimental results showed that the proposed algorithm has kept a very low false alarm rate and extremely high detection rate.

Keywords: Target Spectrum Signature Detection, Multi-frame Acoustic Signal Processing, Time-Frequency Domain, Adaptive Constant False Alarm Rate (ACFAR).

1. INTRODUCTION

For the urgent needs of China's national defense and ocean defense in the coastal areas, the deployment of deep-sea underwater sonar detection system network, will greatly enhance the ability of monitoring and controlling of various kind of ships, including unmanned ships and submarine activities in China Sea. The establishment of sonar detection network system can weaken the combat capability of foreign underwater ships and submarines in many ways, which is the foundation of the concept of Airsea battle. Moreover, if the sonar real-time detection system can be deployed to the Yellow Sea, South China Sea and East China sea bottom, and can be linked as a network, the unexpected marine vehicles, such as submarine can only stay outside of the network coverage. This will greatly weaken the foreign troops in the conflict in the coastal areas near main land China.

With the increase of unauthorized arrivals, drug smugglers, illegal fishing and a range of other border threats the border protection becomes more and more important to the international community. An alarming system which can detect and report the existence of alien marine vehicles is becoming an urgent task for the authority.

The author is targeting the applications on these aspects by successfully developed a very effective acoustic signal detection algorithm, which can be used for detection and monitoring of illegal activities on the wide range of coastlines by detecting any unexpected marine vehicles by means acoustic techniques [1]-[7].

This paper is focused on the theoretical algorithms development and experimental research of automatic detection of acoustic signals, especially for boat generated signals by hydrophone [8]-[14]. In this paper, an observation space is created by dividing input acoustic signals into multiple frames, and each frame is sampled and transformed into the frequency domain. The multiple frame signal processing algorithm is proposed in this paper for the purpose of increasing the probability of final detection. Some samples of the observation space are shown in Fig. 1, in

which, the horizontal axis is frequency in Hz, and vertical is time in seconds (or number of frames). We can also see that there are not only the vertical frequency strips that are generated by marine vehicles, but also some curved strips that are caused by multi-path effects due to shallow water environment.

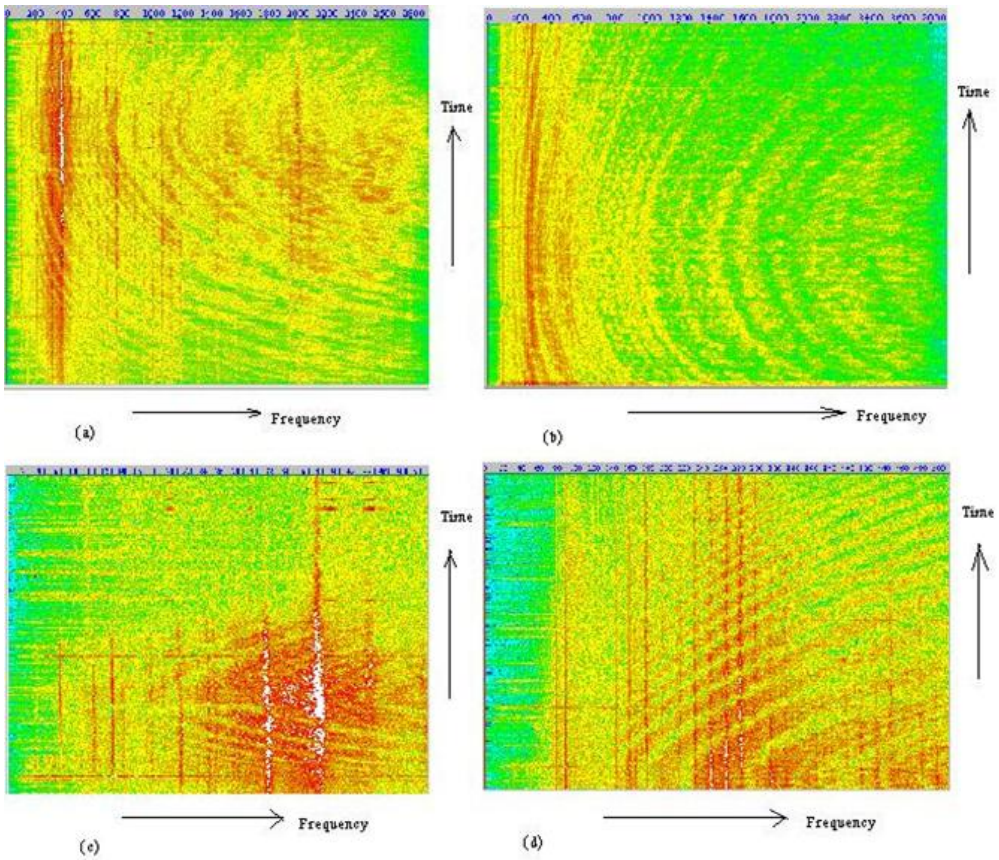

FIGURE 1: Samples of Observation Space (Time and frequency space).

The concept of Constant False Alarm Rate and its application had been used in radar system for a long time [15]-[25]. But there is no appropriate CFAR algorithm was proposed in sonar system, especially for the practical applications. In this paper, an Adaptive Median Constant False Alarm Rate (MCFAR) algorithm in time-frequency domain has been proposed for automatic detection of boat generated acoustic signals in each frame, in which a low constant false alarm rate is kept with relatively high detection rate first. Then, a post detection fusion algorithm with time (or number of frames) is proposed to increase probability of final detection and make the whole detection more robust. The proposed algorithms have been tested on real acoustic signals received and recorded from hydrophone, which were generated by real marine vehicles, called 'Kimbla', 'Ferry', 'Naiad1', 'Naiad2', 'Reef heron1', 'Reef heron2' and 'Kuala Lumpur'.

2. OPTIMUM DETECTION STRUCTURE UNDER THE NEYMAN-PEARSON CRITERION

2.1 Optimum detection structure under the Neyman-Pearson criterion for a single bin in a given frame and a frequency bin

The acoustic signal detection and multi-frame fusion algorithms proposed in this paper are structured based on the Neyman-Pearson (NP) criterion [26]-[30]. This criterion is suitable for target detection application either in sonar or radar systems. The observation space of the

detector is shown in Fig. 2, in which horizontal direction represent frequency (number of frequency bins), and vertical direction represent time (number of frames).

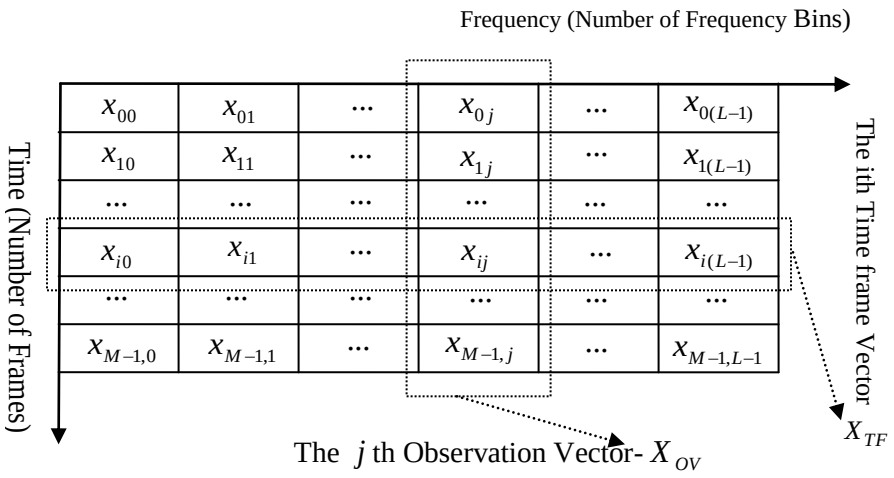

FIGURE 2: Observation Space for The Acoustic Signal Neyman-Pearson Detector.

The following analysis is based on the signal in the frequency domain [31]-[32], in i th frame and j th frequency bin. The hypothesis test assumes:

$$H_0 : x_{i,j} = n_{i,j},$$
$$H_1 : x_{i,j} = s_{i,j} + n_{i,j}. \quad (1)$$

Where n_i is the noise sample in i th frame and j th frequency bin, s_i is the signal sample in i th frame and j th frequency bin, in which $i = 0,1,...,M-1$ is the index of frames in the proposed algorithm.

We assume that the noise in all frequency bins are independent and has the same Gaussian probability distribution with the mean μ_N and variance σ_N^2, i.e. $n_{i,j} \in N(\mu_N, \sigma_N^2)$. The signal $S_{i,j}$ in all different frequency bins are non-random constants. These assumptions are quite true for the short period of observation of 15 to 20 seconds.

In H_0 hypothesis, we assume that the received digital signals in i th frame and j th frequency bin only contain noise. In H_1 hypothesis, we assume that the received digital sequences in i th frame and j th frequency bin contain signal and noise.

Thus, the probability distribution function (pdf) of $x_{i,j}$ under the hypothesis H_0, is shown in equation (2).

$$p_0(x_{i,j}) = \frac{1}{\sqrt{2\pi}\sigma_N} \exp[-\frac{(x_{i,j} - \mu_N)^2}{2\sigma_N^2}] \quad (2)$$

Similarly, the probability distribution function (pdf) of $x_{i,j}$, under the hypothesis H_1, is shown in equation (3).

$$p_0(x_{i,j}) = \frac{1}{\sqrt{2\pi}\sigma_N} \exp[-\frac{(x_{i,j} - S_{i,j} - \mu_N)^2}{2\sigma_N^2}] \quad (3)$$

In order to keep a constant false alarm rate and maximize the signal detection probability in each frequency bin, a Median CFAR algorithm is proposed in the paper, which will be described in section 4. In which a floating threshold $x_{i,j}^{median}$ is the median value of the frequency bins that are covered by a sliding window, i.e.

$$x_{i,j}^{median} = Median\{x_{i,j-k}, x_{i,j-k+1}, \Lambda, x_{i,j}, x_{i,j+1}, \Lambda, x_{i,j+k}\} \quad (4)$$

The Median filter size is $(2k+1)$, in which $k = 1,2,3$.
We assume the median window size is big enough to exclude the existent signal in i th frame and j th frequency bin, so the $x_{i,j}^{median}$ is an accurate estimate of the neighborhood noise. So, the probability distribution function (pdf) of the $x_{i,j}^{median}$ in different frames and frequency bins also has a Gaussian probability distribution with the mean μ_N and the variance σ_N^2, i.e.

$$p(x_{i,j}^{median}) = \frac{1}{\sqrt{2\pi}\sigma_N} \exp[-\frac{(x_{i,j}^{median} - \mu_N)^2}{2\sigma_N^2}] \quad (5)$$

Hence, the hypothesis after Median CFAR operation becomes

$$\begin{aligned} H_0 &: \hat{x}_{ij} = x_{i,j} - x_{i,j}^{median} = n_{i,j} - n_{i,j}^{median}, \\ H_1 &: \hat{x}_{ij} = x_{i,j} - x_{i,j}^{median} = s_{i,j} + n_{i,j} - n_{i,j}^{median}. \end{aligned} \quad (6)$$

Based on the law- "the linear combination of independent Gaussian random variables is still a Gaussian random variable [28]". We also know that $x_{i,j}$ under both H_0 and H_1 hypothesis obeys a Gaussian distribution.
So, under the H_0 hypothesis, the mean of $\hat{x}_{i,j}$ is shown in equation (7).

$$E\{\hat{x}_{i,j}\} = E\{n_{i,j} - n_{i,j}^{median}\} = E\{n_{i,j}\} - E\{n_{i,j}^{median}\} = \mu_N - \mu_N = 0, \quad (7)$$

The variance of $\hat{x}_{i,j}$ is calculated and shown in equation (8).

$$\begin{aligned} &\sigma_{\hat{x}_{i,j}}^2 = E\{(\hat{x}_{i,j} - E\{\hat{x}_{i,j}\})^2\} = E\{(n_{i,j} - n_{i,j}^{median} - E\{n_{i,j}\} + E\{n_{i,j}^{median}\})^2\} \\ &= E\{(n_{i,j} - E\{n_{i,j}\})^2\} - 2E\{(n_{i,j} - E\{n_{i,j}\})(n_{i,j}^{median} - E\{n_{i,j}^{median}\})\} + E\{(n_{i,j}^{median} - E\{n_{i,j}^{median}\})^2\} \end{aligned} \quad (8)$$

Since $n_{i,j}$ and $n_{i,j}^{median}$ are independent,

$$E\{(n_{i,j} - E\{n_{i,j}\})(n_{i,j}^{median} - E\{n_{i,j}^{median}\})\} = 0, \quad (9)$$

The equation (8) becomes,

$$\begin{aligned} &\sigma_{\hat{x}_{i,j}}^2 = E\{(n_{i,j} - E\{n_{i,j}\})^2\} + E\{(n_{i,j}^{median} - E\{n_{i,j}^{median}\})^2\} \\ &= \sigma_N^2 + \sigma_N^2 = 2\sigma_N^2 \end{aligned} \quad (10)$$

Thus, the probability distribution of $\hat{x}_{i,j}$ under H_0 is shown in equation (11).

$$p_0(\hat{x}_{i,j}) = \frac{1}{\sqrt{4\pi}\sigma_N} \exp[-\frac{(\hat{x}_{i,j})^2}{4\sigma_N^2}] \quad (11)$$

Similarly, under the H_1 hypothesis,
The mean $\hat{x}_{i,j}$ is shown in equation (12).

$$E\{\hat{x}_{i,j}\} = E\{s_{i,j} + n_{i,j} - n_{i,j}^{median}\} = s_{i,j} \quad (12)$$

The variance of $\hat{x}_{i,j}$ is calculated and shown in equation (13).

$$\begin{aligned} \sigma^2_{\hat{x}_{i,j}} &= E\{(\hat{x}_{i,j} - E\{\hat{x}_{i,j}\})^2\} \\ &= E\{(s_{i.j} + n_{i,j} - n_{i,j}^{median} - s_{i,j})^2\} \\ &= 2\sigma_N^2 \end{aligned} \quad (13)$$

So, the probability distribution of $\hat{x}_{i,j}$ under H_1 hypothesis is shown in equation (14).

$$p_1(\hat{x}_{i,j}) = \frac{1}{\sqrt{4\pi}\sigma_N} \exp[-\frac{(\hat{x}_{i,j} - s_{i,j})^2}{4\sigma_N^2}] \quad (14)$$

The pictures of $p_0(\hat{x}_{i,j})$ and $p_1(\hat{x}_{i,j})$ are shown in Fig. 3.

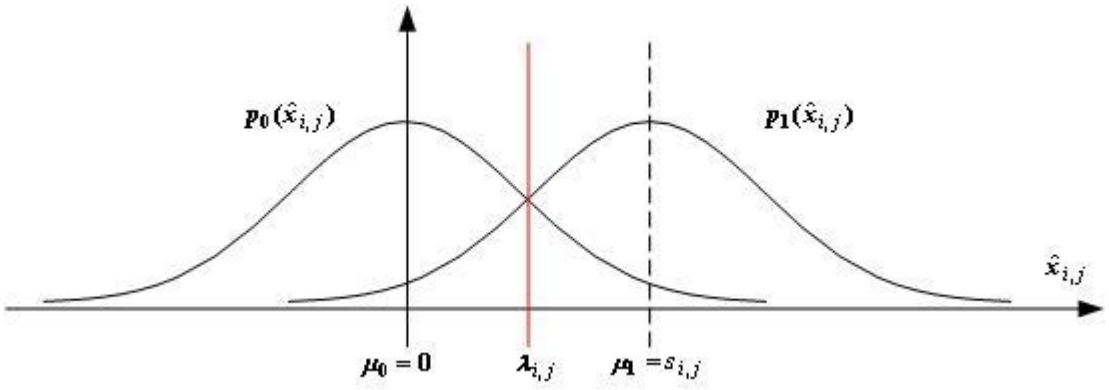

FIGURE 3: Probability distributions of $p_0(\hat{x}_{i,j})$ and $p_1(\hat{x}_{i,j})$ after Median CFAR operation

Since in the passive sonar applications, we do not know the priori probabilities $P(H_0)$ and $P(H_1)$, but we know the probability distribution (pdf s) of signal and noise. In this case, Neyman-Pearson (NP) is applied, in which under the specified constant false alarm rate $P_{fa}(i,j)$, the probability of detection $P_D(i,j)$ is maximized.

In Fig. 3, the probability of false alarm detection of the given bin - $P_{fa}(i,j)$ is the area of the

function $p_0(\hat{x}_{i,j})$ above the detection threshold - $\lambda_{i,j}$, i.e.

$$P_{fa}(i,j) = \int_{\lambda_{i,j}}^{\infty} p_0(\hat{x}_{i,j})d\hat{x}_{i,j} = \int_{\lambda_{i,j}}^{\infty} \frac{1}{\sqrt{4\pi}\sigma_N} \exp[-\frac{(\hat{x}_{i,j})^2}{4\sigma_N^2}]d\hat{x}_{i,j} = \alpha_{i,j} \quad (15)$$

The probability of the detection of the given bin - $P_D(i.j)$ is the area of the function $p_1(\hat{x}_{i,j})$ above the detection threshold - $\lambda_{i,j}$, i.e.

$$P_D(i,j) = \int_{\lambda_{i,j}}^{\infty} p_1(\hat{x}_{i,j})d\hat{x}_{i,j} = \int_{\lambda_{i,j}}^{\infty} \frac{1}{\sqrt{4\pi}\sigma_N} \exp[-\frac{(\hat{x}_{i,j} - s_{i,j})^2}{4\sigma_N^2}]d\hat{x}_{i,j} = \beta_{i,j} \quad (16)$$

Based on the Neyman-Pearson criterion, the goal of keeping the false alarm rate $P_{fa}(i,j)$ in an acceptable level, and maximizing the detection rate $P_D(i.j)$ can be achieved by using a likelihood rate test (LRT) [26].
The likelihood rate test of the above hypothesis can be represented as:

$$H_0 : \Lambda(\hat{x}_{i,j}) = \frac{p_1(\hat{x}_{i,j})}{p_0(\hat{x}_{i,j})} < \eta_{i,j}$$
$$H_1 : \Lambda(\hat{x}_{i,j}) = \frac{p_1(\hat{x}_{i,j})}{p_0(\hat{x}_{i,j})} \geq \eta_{i,j} \quad (17)$$

Replacing $p_0(\hat{x}_{i,j})$ and $p_1(\hat{x}_{i,j})$ with equations (11) and (14), we can obtain the likelihood rate, which is shown in equation (18).

$$\Lambda(\hat{x}_{i,j}) = \frac{p_1(\hat{x}_{i,j})}{p_0(\hat{x}_{i,j})} = \exp\{-\frac{(\hat{x}_{i,j} - s_{i,j})^2}{4\sigma_N^2} + \frac{(\hat{x}_{i,j})^2}{4\sigma_N^2}\} = \exp\{\frac{s_{i,j}(2\hat{x}_{i,j} - s_{i,j})}{4\sigma_N^2}\} \quad (18)$$

Thus, the likelihood rate test shown in equation (17) can be simplified by replacing with equation (18),

$$H_0 : \hat{x}_{i,j} < \frac{[s_{i,j}^2 + 4\sigma_N^2 \ln(\eta_{i,j})]}{2s_{i,j}}$$
$$H_1 : \hat{x}_{i,j} \geq \frac{[s_{i,j}^2 + 4\sigma_N^2 \ln(\eta_{i,j})]}{2s_{i,j}} \quad (19)$$

Then, the optimum threshold $\lambda_{i,j}$ can be represented in the following equation:

$$\lambda_{i,j} = \frac{[s_{i,j}^2 + 4\sigma_N^2 \ln(\eta_{i,j})]}{2s_{i,j}} \quad (20)$$

If we assume that the signal strength and noise (or clutter) level are constant in all bins in different frames during the observation period, (This is quite true for the 15 to 20 seconds observation time.) the optimum threshold is also constant for bins during the same observation period, i.e.

$$\lambda = \frac{[s^2 + 4\sigma_N^2 \ln(\eta)]}{2s} = (\frac{s}{2} + \frac{2\sigma_N^2 \ln(\eta)}{s}) \tag{21}$$

We can see that the optimum detection threshold is a function of the signal strength s and the noise level σ_N^2 .

2.2 Detector Performance Measurement After Post-Detection Fusion

The post-detection fusion algorithm after single frame detection is described in Section 3, in equations (32) to (37).

The output of single frame detection can be described in the following vector,

$$Y = [y_0, y_1, \Lambda\ , y_j, \Lambda\ , y_{(L-1)}] \tag{22}$$

Where the output of *j* th bin is represented in equation (23).

$$y_j = \sum_{i=0}^{M-1} y_{i,j} \tag{23}$$

Where the $y_{i,j}$ is shown in equation (24).

$$y_{ij} = \begin{cases} 1, & (x_{i,j} - x_{i,j}^{median}) \geq \lambda_{i,j} \\ 0, & otherwise \end{cases} \tag{24}$$

In order to calculate the performance of our detector, we need to calculate the following probabilities.

Since $y_{i,j}$ can be treated as a binary random variable, the probability of $y_{i,j} = 1$ is shown in equation (25).

$$\begin{aligned} &P[y_{i,j} = 1] \\ &= P[(x_{i,j} - x_{i,j}^{median}) > \lambda_{i,j}] \\ &= P(H_0)P_{fa}(i,j) + P(H_1)P_D(i,j) \end{aligned} \tag{25}$$

Replace equations (15) and (16) in equation (25), we obtain,

$$P[y_{i,j} = 1] = P(H_0)\int_{\lambda_{i,j}}^{\infty} \frac{1}{\sqrt{4\pi}\sigma_N} \exp[-\frac{(\hat{x}_{i,j})^2}{4\sigma_N^2}]d\hat{x}_{i,j} + P(H_1)\int_{\lambda_{i,j}}^{\infty} \frac{1}{\sqrt{4\pi}\sigma_N} \exp[-\frac{(\hat{x}_{i,j} - s_{i,j})^2}{4\sigma_N^2}]d\hat{x}_{i,j}$$

(26)

Similarly, we can obtain,

$$P[y_{i,j}=0]=P(H_0)\int_{-\infty}^{\lambda_{i,j}}\frac{1}{\sqrt{4\pi}\sigma_N}\exp[-\frac{(\hat{x}_{i,j})^2}{4\sigma_N^2}]d\hat{x}_{i,j}+P(H_1)\int_{-\infty}^{\lambda_{i,j}}\frac{1}{\sqrt{4\pi}\sigma_N}\exp[-\frac{(\hat{x}_{i,j}-s_{i,j})^2}{4\sigma_N^2}]d\hat{x}_{i,j}$$

(27)

So, the probability of *k* (*k=0, 1, 2, …,M*) bins successfully detected in *M* frames in *j* th frequency bins is calculated in the following equation.

$$\begin{aligned}&P[y_j=k]=P[\sum_{i=0}^{M-1}y_{i,j}=k]\\&=C_M^k\{P[y_{i,j}=1]\}^k\{P[y_{i,j}=0]\}^{M-k}\\&=\frac{M!}{k!(M-k)!}\{P(H_0)\int_{\lambda_{i,j}}^{\infty}\frac{1}{\sqrt{4\pi}\sigma_N}\exp[-\frac{(\hat{x}_{i,j})^2}{4\sigma_N^2}]d\hat{x}_{i,j}+P(H_1)\int_{\lambda_{i,j}}^{\infty}\frac{1}{\sqrt{4\pi}\sigma_N}\exp[-\frac{(\hat{x}_{i,j}-s_{i,j})^2}{4\sigma_N^2}]d\hat{x}_{i,j}\}^k\cdot\\&\{P(H_0)\int_{-\infty}^{\lambda_{i,j}}\frac{1}{\sqrt{4\pi}\sigma_N}\exp[-\frac{(\hat{x}_{i,j})^2}{4\sigma_N^2}]d\hat{x}_{i,j}+P(H_1)\int_{-\infty}^{\lambda_{i,j}}\frac{1}{\sqrt{4\pi}\sigma_N}\exp[-\frac{(\hat{x}_{i,j}-s_{i,j})^2}{4\sigma_N^2}]d\hat{x}_{i,j}\}^{M-k}\end{aligned}$$

(28)

Thus, the probability of detection in *j* th bin after post-detection fusion can be calculated as follows.

$$\begin{aligned}&P_D(j)=P[y_j>\lambda_j]\\&=\sum_{k=0}^{\lambda_j}P[y_j=k]\\&=\sum_{k=0}^{\lambda_j}\frac{M!}{k!(M-k)!}\{P(H_0)\int_{\lambda_{i,j}}^{\infty}\frac{1}{\sqrt{4\pi}\sigma_N}\exp[-\frac{(\hat{x}_{i,j})^2}{4\sigma_N^2}]d\hat{x}_{i,j}+P(H_1)\int_{\lambda_{i,j}}^{\infty}\frac{1}{\sqrt{4\pi}\sigma_N}\exp[-\frac{(\hat{x}_{i,j}-s_{i,j})^2}{4\sigma_N^2}]d\hat{x}_{i,j}\}^k\cdot\\&\{P(H_0)\int_{-\infty}^{\lambda_{i,j}}\frac{1}{\sqrt{4\pi}\sigma_N}\exp[-\frac{(\hat{x}_{i,j})^2}{4\sigma_N^2}]d\hat{x}_{i,j}+P(H_1)\int_{-\infty}^{\lambda_{i,j}}\frac{1}{\sqrt{4\pi}\sigma_N}\exp[-\frac{(\hat{x}_{i,j}-s_{i,j})^2}{4\sigma_N^2}]d\hat{x}_{i,j}\}^{M-k}\end{aligned}$$

(29)

Where λ_j is the final detection threshold, and its value is in the range of *0* to *M*.

The false alarm rate in the detection of in *j* th bin after post-detection fusion can be given in equation (30).

$$\begin{aligned}&P_{fa}(j)=1-P_D(j)\\&=1-\sum_{k=0}^{\lambda_j}\frac{M!}{k!(M-k)!}\{P(H_0)\int_{\lambda_{i,j}}^{\infty}\frac{1}{\sqrt{4\pi}\sigma_N}\exp[-\frac{(\hat{x}_{i,j})^2}{4\sigma_N^2}]d\hat{x}_{i,j}+P(H_1)\int_{\lambda_{i,j}}^{\infty}\frac{1}{\sqrt{4\pi}\sigma_N}\exp[-\frac{(\hat{x}_{i,j}-s_{i,j})^2}{4\sigma_N^2}]d\hat{x}_{i,j}\}^k\cdot\\&\{P(H_0)\int_{-\infty}^{\lambda_{i,j}}\frac{1}{\sqrt{4\pi}\sigma_N}\exp[-\frac{(\hat{x}_{i,j})^2}{4\sigma_N^2}]d\hat{x}_{i,j}+P(H_1)\int_{-\infty}^{\lambda_{i,j}}\frac{1}{\sqrt{4\pi}\sigma_N}\exp[-\frac{(\hat{x}_{i,j}-s_{i,j})^2}{4\sigma_N^2}]d\hat{x}_{i,j}\}^{M-k}\end{aligned}$$

(30)

Based on equations (29) and (30), we can see that both probabilities of detection and false alarm rate of our detector after post-detection fusion are the functions of signal strength, noise power, (i.e. SNR), probability threshold (λ_j / M), fusion frame number (*M*) and potential function of Median CFAR window length.

3. MULTI-FRAME ACOUSTIC SIGNAL PROCESSING AND DETECTION ALGORITHM IN THE FREQUENCY DOMAIN

A multi-frame acoustic signal processing and detection algorithms in the frequency domain are proposed in this paper, as summarized in Fig. 4.

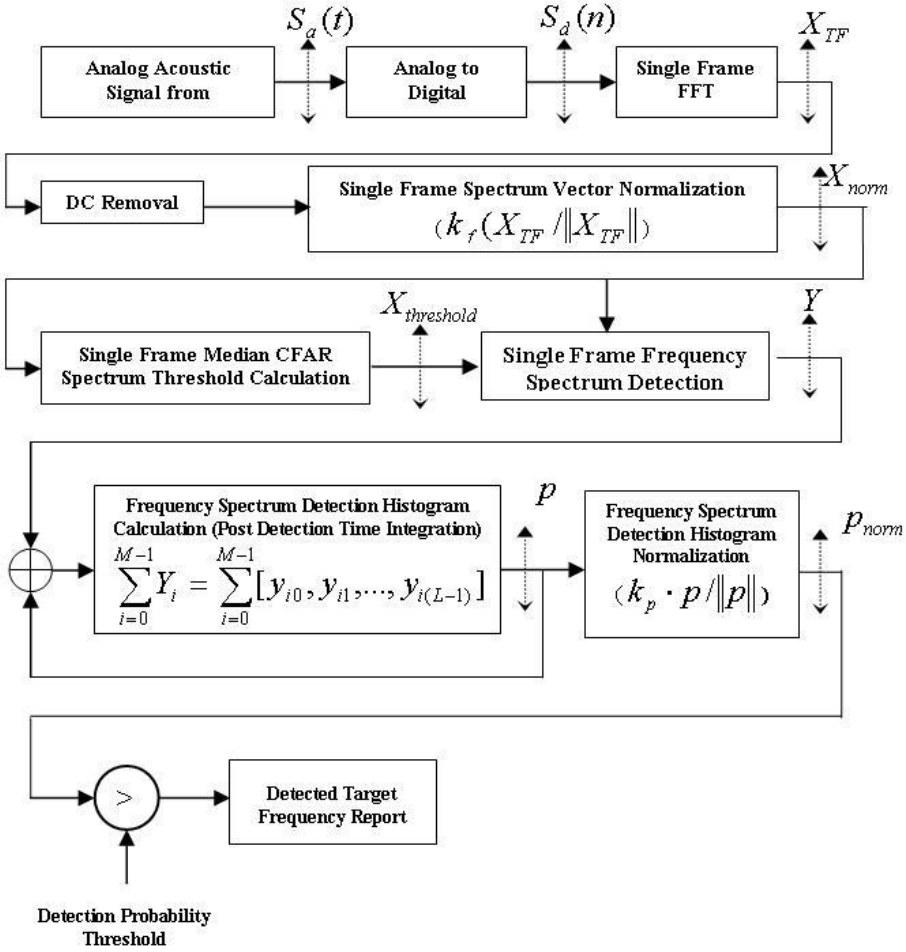

FIGURE 4: Multi-Frame Acoustic Signal Processing and Detection Algorithm.

Acoustic signals from hydrophone are converted into digital signals based on the Nyquist Sampling Theorem (Criterion) [33]-[38], imposing a sampling rate larger than twice the maximum signal frequency. In our experiments, we used a sampling rate of 2048 Hz, so the maximum frequency we are interested is 1024 Hz. Then, the digital signal (converted from analog input signal) is divided into frames. Each frame lasts T seconds, and in our experiments the T was chosen as 0.5 seconds with the sampling rate 2048 Hz, so the data processing period in digital format is N=1024.

In order to detect acoustic signal (typically boat generated signals), the digital signals need to be transformed into the frequency domain frame by frame. In our experiment, the digital signals are transformed into the frequency domain by using FFT, which is the fastest and most effective algorithm for Digital Fourier Transform (DFT). Since the data processing period in digital format is 1024 in our experiment, we choose the same length as FFT length, which is also 1024 points.

Some frame pre-processing in the frequency domain is necessary before we start detecting signal frequencies, which includes DC removal and spectrum frame vector normalization. DC removal is required because all acoustic signals have a DC component (sometimes very strong),

which is not part of the signal generated by a target boat, but can affect our target frequency components detection results. The DC component is removed, also because it does not carry any useful information.

In order to deal with various input signal strength and make the whole automatic detection robust, 'single frame spectrum magnitude normalization' is performed in the frequency domain. At this stage, each element in the frame vector is divided by the magnitude of the vector (geometric length). After normalization, a magnitude amplification of 40 dB (100 times) is used to give the signal a reasonable dynamic value range.

The single frame spectrum vector is normalized by its vector length, which is described as follows,

$$X_{norm}^{i} = k_f \cdot X_{TF} \Big/ \|X_{TF}\| = k_f \cdot \frac{\left[x_{i0}, x_{i1}, \Lambda, x_{i(L-1)}\right]^T}{\sqrt{x_{i0}^2 + x_{i1}^2 + \Lambda + x_{i(L-1)}^2}} \tag{31}$$

In which i is frame index, and k_f is a scaling factor that keep the whole vector in a reasonable dynamic range, in our experiments, k_f is chosen as 40 dB.

Then, an adaptive median CFAR algorithm is proposed to calculate the Constant False Alarm Rate threshold in a single frame, in which the threshold for each frequency bin is the median value of its sliding window. After that, the input signal spectrum is compared with the CFAR threshold, and if the difference is bigger than a constant threshold λ , it is reported as target frequency, otherwise it is treated as background noise. The $1/\lambda$ is called sensitivity of our detection system. The bigger the λ is, the less sensitive is our detection system. Since the CFAR threshold in each bin is calculated based on its neighborhood noise, it will keep our automatic detection system at low and constant false alarm rate.

The Adaptive Median Constant False Alarm Rate (Adaptive Median CFAR) threshold vector X_i^{median} is calculated by passing X_i^{norm} into a Median filter (Where the i is the frame index, and the properties and size of this filter will be discussed in the next section.), which is

$$X_i^{median} = [x_{i,0}^{median}, x_{i,1}^{median}, \Lambda, x_{i,j}^{median}, \Lambda, x_{i,L-1}^{median}]^T \tag{32}$$

Where i is the frame index, and $j = 0,1,\Lambda, L-1$ is the frequency bin index, and each threshold element is,

$$x_{i,j}^{median} = Median\left\{x_{i,j-k}^{norm}, x_{i,j-k+1}^{norm}, \Lambda, x_{i,j}^{norm}, x_{i,j+1}^{norm}, \Lambda, x_{i,j+k}^{norm}\right\} \tag{33}$$

In which, the Median filter size is $(2k+1)$, and $k = 1,2,3$. And the single frame detection result is a binary vector, which is based on the comparison of the vectors X_i^{norm} and X_i^{median}, and the output is shown in equation (34),

$$Y_i = \left[y_{i0}, y_{i1}, \Lambda, y_{i(L-1)}\right]^T \tag{34}$$

Where the i is the frame index, the j is the frequency bin index, and $y_{ij}\,(j = 0,1,\Lambda, L-1)$ is single frame detection output, which is,

$$y_{ij} = \begin{cases} 1, \left(x_{i,j}^{norm} - x_{i,j}^{threshold}\right) \geq \lambda \\ 0, otherwise \end{cases} \tag{35}$$

where λ is a constant threshold, and $1/\lambda$ is called sensitivity in our experiments. The smaller the λ , the more sensitive is our detector.

Based on the Neyman-Pearson criterion, the most important aspect in target frequency components detection is to increase the probability of detection. Accordingly, the fusion of single frame detection results over time (i.e. over a number of frames) was used to increase the final detection probability. A typical value of fusion time for sonar buoy acquired signals is about 15 seconds, which is corresponds to about 15 frames in our testing system.

The 'Integrated Detection vector' is,

$$p = [p_0, p_1, \Lambda, p_{(L-1)}] = \sum_{i=0}^{M-1} Y_i = \sum_{i=0}^{M-1} [y_{i0}, y_{i1}, \cdots, y_{i(L-1)}] \quad (36)$$

The p vector is a description of the frequency (or times) of single frame detection of each frequency bin, and final detection is based on the distribution function. In order to make the performance of the detection system more robust, especially for weak signals, the 'Integrated Detection Vector' is normalized by its geometric magnitude ($p/\|p\|$) and amplified by a scaling factor k_p (40 dB), in which the final detection will be more robust and reliable.

4. MEDIAN CONSTANT FALSE ALARM RATE DETECTION ALGORITHM IN THE FREQUENCY DOMAIN

Based on the Neyman-Person criterion, in order to reduce false alarm rate during the target signal detection, an adaptive median CFAR algorithm is proposed in this paper, in which acoustic target signals are detected with a low false alarm and relative high detection rates in the frequency domain. The first step is to transform input acoustic signals into the frequency domain by using FFT, then, an optimizes algorithm will be used to detect target generated frequency components. The basic idea of the proposed algorithm is that for each frequency bin, use different adaptive CFAR (Constant False Alarm Rate) thresholds rather than a single, constant threshold (which is often the case in acoustic systems) [24]-[33]**.** The threshold of each frequency bin is based on its surrounding background noise. The higher the background noise, the higher the threshold is set. To the best of our knowledge, while this idea is often used in radar system to obtain lower false alarm rate with relatively higher target detection rate, it is applied here for the first time to sonar-generated acoustic signals, especially for the proposed Median CFAR algorithm. Moreover, the Median CFAR algorithm uses a Median Filter Window centered around each frequency bin to calculate the threshold value for the input signals.

Since the median filter is good at removing high frequency spike noise, it is a very good way to calculate threshold vector without being affected by existent signals. The relationship between input signal spectrum vector and its threshold vector is same as passing an input signal spectrum into a Median Filter (in frequency domain), and output signal is our threshold vector, which is shown in Figure 5.

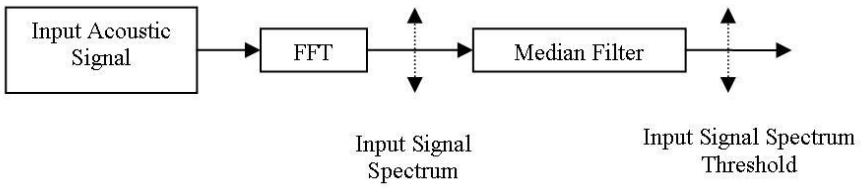

FIGURE 5: Relationships Among Input Acoustic Signal, Its Spectrum And Threshold.

The Adaptive Median CFAR algorithm is superior over the Average CFAR algorithm, since in the Average CFAR algorithm every pixel in the averaging window will affect the threshold, especially when the signal or a noise spike is strong. The major advantage of the Median filter is its ability to remove interference such as a strong signal or noise spikes without affecting the sharpness of edges retaining sharp edges after filtering. Conversely, with an averaging LPF (low pass filter), which is equivalent to the Average CFAR algorithm, sharp edges will be blurred after filtering. The strong signal is a major interference, affecting its accuracy when calculating the threshold. Further evidence of the superiority of the median filter with respect to average filters for the description of the background process can be found in [26]-[31].

The size of Median Filter window is an odd number, which can be $3,5,7,\Lambda\ ,(2k+1)$. The principle of the Median CFAR algorithm is illustrated in Fig. 6 by using a window size of 5, which has been proved to be appropriate in our experimental application.

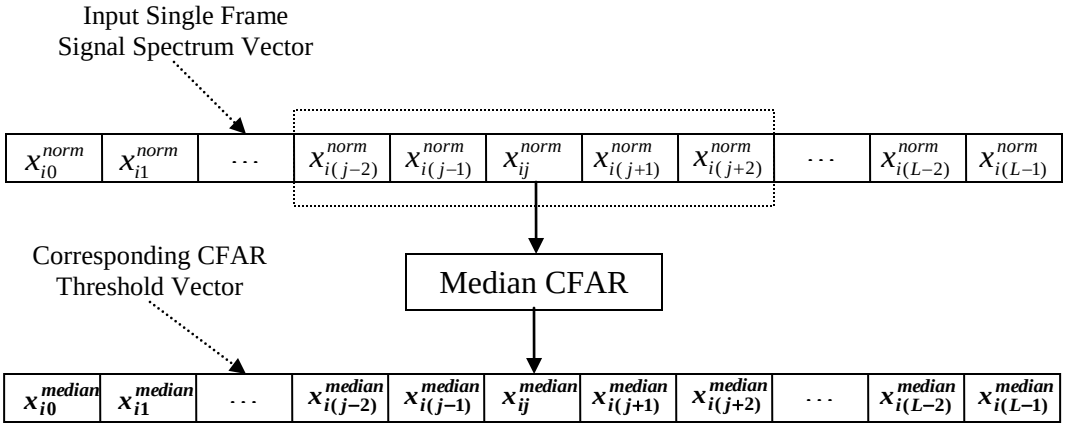

FIGURE 6: Median CFAR Algorithm Principle.

The threshold vector is calculated by passing a sliding window through the input frequency vector. Each threshold is the median value of the frequency bins that are covered by sliding window. As is shown in Fig. 6, the threshold of the *i*th frame and jth frequency bin with the proposed Median CFAR window size of *(2k+1)*, is shown in equation (37).

$$x_{ij}^{median} = Median\left\{x_{i(j-k)}^{norm},\Lambda\ , x_{i(j-1)}^{norm}, x_{ij}^{norm}, x_{i(j+1)}^{norm},\Lambda\ , x_{i(j+k)}^{norm}\right\} \tag{37}$$

Where $i=0,1,2,\Lambda\ ,(M-1)$ is index of frames, $j=0,1,2,\Lambda\ ,(j-2),(j-1),j,(j+1),(j+2),\Lambda\ ,(L-1)$ is the frequency bin number, L is the single frame vector length in frequency domain and is also the FFT length, and the window size is $(2k+1)$. And in order to deal with edge pixel situation, both input signal spectrum vector and threshold vector are treated as wrapped period signals.

The proposed adaptive CFAR (Constant False Alarm Rate) algorithm is used to detect targets generated frequency components with relatively high detection rate while maintaining a low and constant false alarm rate. The size of the Median window has to be an odd number, which has an effect on the output threshold signal. In the experimentation 3, 5 and 7 have been chosen. The impact of the window size is shown in Figure 10, where it can be seen that the larger the window size, the lower frequency components exist on the output threshold image.

5. EXPERIMENTAL RESULTS WITH THE PROPOSED MEDIAN CFAR AND MULTI-FRAME FUSION ALGORITHM IN THE FREQUENCY DOMAIN

The test signals are provided by Soncom PTY LTD, which are from 'C-Buoy/Off-Buoy Processor Sea Trials' at Low Islets on 17 June, 2002 in Australia. These real sonar signals are original

sampled at sampling rate of 44100 Hz, and down sampled into 2205 Hz, in order to meet our target detection experimental purposes. These acoustic signals generated by marine vehicles are called ‘Kimbla’, ‘Ferry’, ‘Naiad1’, ‘Naiad2’, ‘Reef heron1’, ‘Reef heron2’ and ‘Kuala Lumpur’ for the following reference.

5.1 Median CFAR Algorithm Single Frame Acoustic Signal Detection Test

The proposed Median CFAR algorithm has been tested on single frame real acoustic signal, which is shown in Fig. 7(a). We can see that there is a very strong signal component located about 160 Hz (the strength is about 23 dB.), and there are also some harmonic frequency components around 1000 Hz, but are much smaller than the main one.

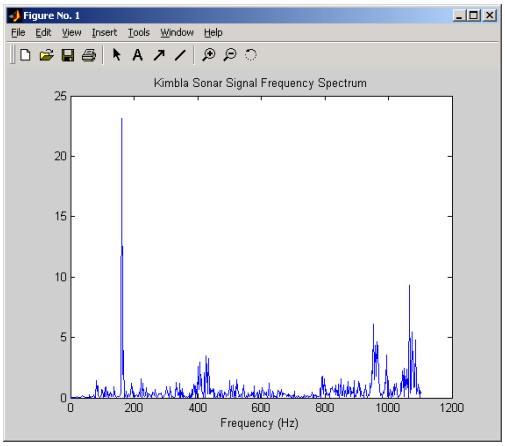

(a) ‘Kimbla’ boat single frame signal spectrum

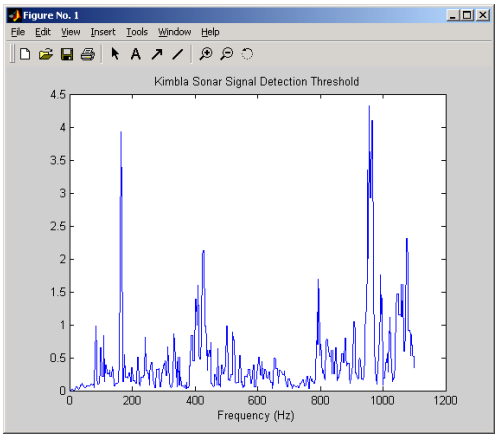

(b) ‘Kimbla’ signal spectrum threshold obtained by applying a Median CFAR Window Size of 3

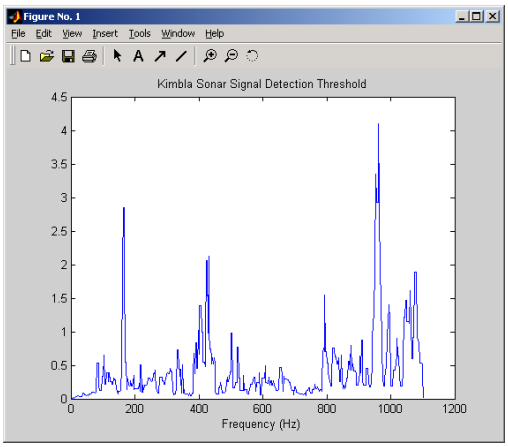

(c) ‘Kimbla’ signal spectrum threshold obtained by applying a Median CFAR Window Size of 5

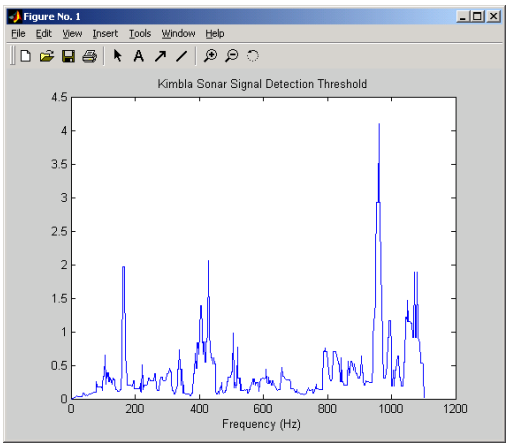

(d) ‘Kimbla’ signal spectrum threshold obtained by applying a Median CFAR window size of 7

FIGURE 7: 'Kimbla' real acoustic signal single frame spectrum and its Median CFAR thresholds.

Fig. 7 (b), (c) and (d) show us the threshold signal spectrum (vector) obtained by applying a Median CFAR window with the window size of 3, 5 and 7 respectively. We can see that the bigger the window size, the smoother is the threshold signal (vector) (less high frequency components). Although there are some spikes in the threshold images, such spikes (less than 4 or 5 dB) are much smaller than signals (about 23 dB). Overall, we can also see that the thresholds in all three cases are all below 4.5 dB in their strength, which are much smaller than the main signal strength

of 23 dB.

The example results of single frame acoustic signal (shown in Fig. 7) detection by using the proposed Median CFAR Algorithm are shown in Fig. 8.

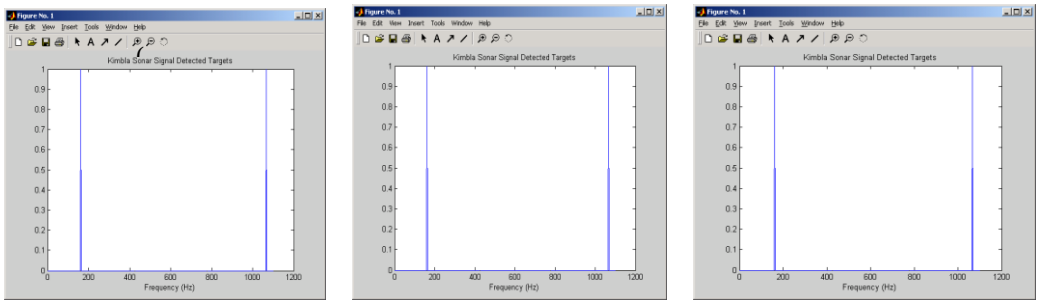

(a) Detected target frequency with Median CFAR algorithm window size of 3 and default sensitivity.

(b) Detected target frequency with Median CFAR algorithm window size of 5 and default sensitivity.

(c) Detected target frequency with Median CFAR algorithm window size of 7 and default sensitivity.

FIGURE 8: 'kimbla' real acoustic signal single frame detection results by using Median CFAR thresholds.

Fig. 8 shows us the detection results of 'Kimbla' single frame signal by using the proposed Median CFAR algorithm, and we can see both the main signal frequency component at about 160 Hz and its harmonic components around 1000Hz are correctly detected by using three different Median CFAR window sizes under the condition of a default sensitivity ($\frac{1}{\lambda}$).

5.2 Multiple Frame Test of Median CFAR Algorithm

The proposed Median CFAR Algorithm has been tested on a multi-frame based 'Kimbla' boat acoustic signal, which is shown in Fig. 9. The effects of Median CFAR window size on the threshold vector, the improvement of final detection after multi-frame fusion have been tested and studied in this section.

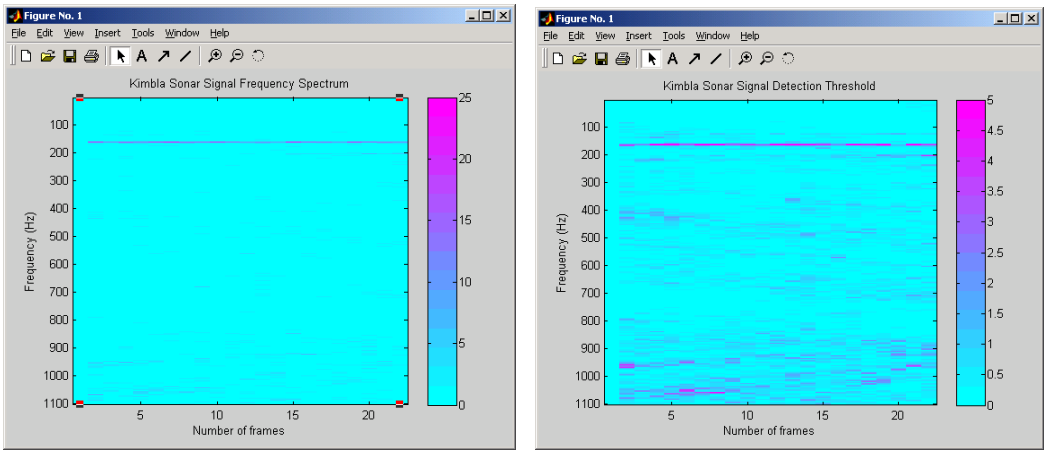

(a) Kimbla boat signal spectrum over multiple frames

(b) Kimbla boat signal spectrum threshold image obtained by applying Median CFAR window size of 3 on original signal spectrum.

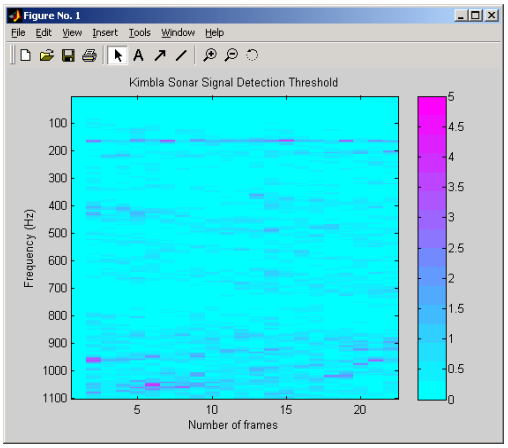

(c) Kimbla boat signal spectrum threshold image obtained by applying a Median CFAR window size of 5 on original signal spectrum.

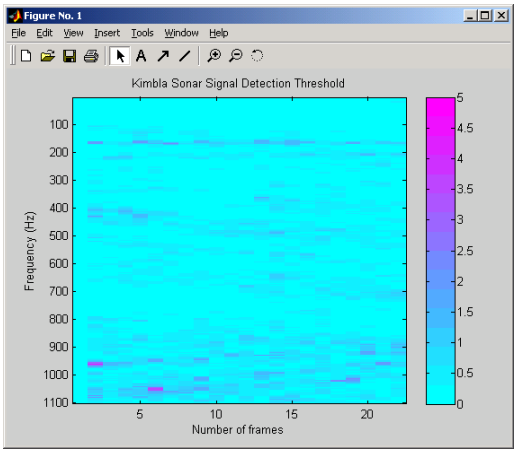

(d) Kimbla boat signal spectrum threshold image obtained by applying a Median CFAR window size of 7 on original signal spectrum.

FIGURE 9: Effect of Median CFAR Window Size On Threshold Signals.

Fig. 9 (a) shows us the 'Kimbla' boat signal spectrum over multiple frames, and Fig. 9 (b), (c) and (d) show us the threshold image signal obtained by using the proposed Median CFAR algorithm with the window sizes of 3, 5 and 7 respectively. We can that the bigger the Median CFAR window, the more blurring of the threshold images.

Example test results of multiple frames detection by using the proposed algorithm are shown in Fig. 10 and Fig. 11, which include original signal spectrum, Median CFAR thresholds image calculated by the proposed algorithm, single frame detection results image and time fusion results.

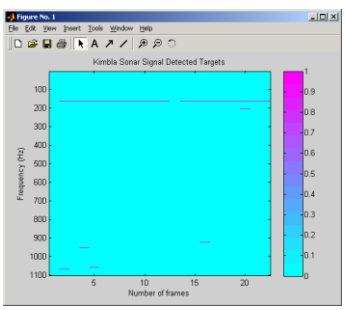

(a) Detected target frequencies by using Median CFAR algorithm with the window size of 3 and default sensitivity.

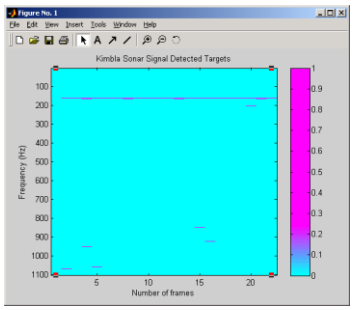

(b) Detected target frequencies by using Median CFAR algorithm with window size of 5 and default sensitivity.

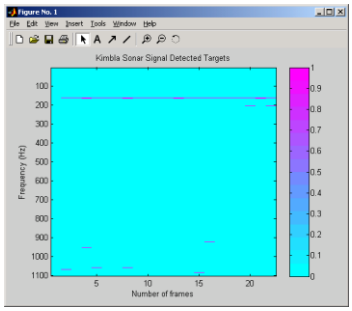

(c) Detected target frequencies by using Media CFAR algorithm with the window size of 7 and default sensitivity.

FIGURE 10: Multiple Frame Target Detection Results

Fig. 10 (a), (b) and (c), show us that the detection results of 'Kimbla' boat acoustic signal by using the Median CFAR algorithm with window size of 3, 5 and 7, respectively, and with the default sensitivity. We can see that with the increase of the window size from 3, 5 to 7, a few more frequency pieces are detected with the bigger window size, i.e. more frequency pieces detected in (c) than (b), and more frequency pieces detected in (b) than (a). Based on the results above, we found out that a Median CFAR window size of 5 was the best in the three test cases, as the boat generated frequency components are correctly detected, but not much noise or harmonic frequency components come in.

The multiple frame fusion results of the signals shown in Fig. 10 are shown in Fig. 11.

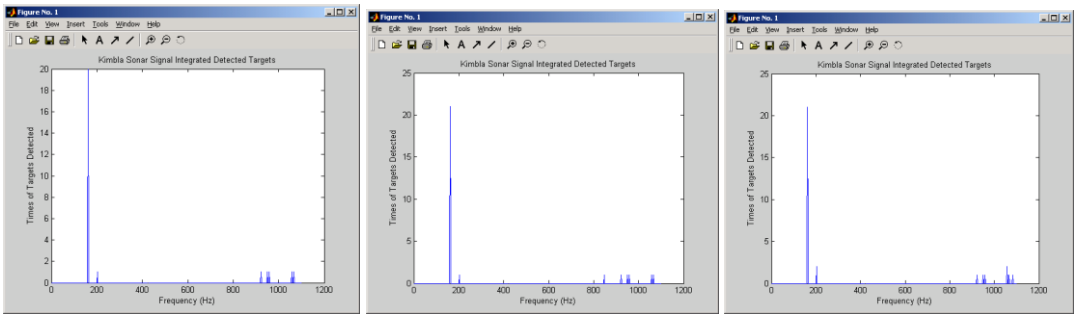

(a) Integrated detected target frequency components with Median CFAR algorithm (window size of 3 and default sensitivity).

(b) Integrated detected target frequency components with Median CFAR algorithm (window size of 5 and default sensitivity)

(c) Integrated detected target frequency components with Median CFAR algorithm (window size of 7 and default sensitivity).

FIGURE 11: Multiple Frame Target Frequency Detection And Fusion Results .

Fig. 11 (a), (b) and (c), show us the fusion-of-detection results on 'Kimbla' boat acoustic signal by using the proposed Median CFAR algorithm with window size of 3, 5 and 7, respectively, and with the default sensitivity. We can see that the correct detection rates of the main frequency component (about 160 Hz in this test case) are 91% (20/22), 96% (21/22) and 96% (21/22) respectively with Fig. 11 (a), (b) and (c). In this case, the size of Median CFAR window will be chosen based on the ability of resistance to interference (existent signal or noise spikes) on its Median CFAR threshold calculation. For example, the Median CFAR Algorithm with the window size of 3 can resist one interference (existent signal or noise spike); the Median CFAR Algorithm with the window size of 5 can resist two interferences, whereas the Median CFAR Algorithm with the window size of 7 can resist three. Based on the analysis above, we believe that overall a Median CFAR window size of 5 is the best trade-off in all these experiments.

5.3 Robust Test of The Proposed Median CFAR and Multi-Frame Fusion Algorithm

The robustness of the proposed Median CFAR and multi-frame fusion has been extensively tested on various different real acoustic signals, which include 'Ferry', 'Naiad1', 'Naiad2', 'Reef heron1', 'Reef heron2' and 'Kuala Lumpur' boat signals, and 'White Gaussian Noise'. The experimental results shown in these tests include signal spectrum image, Median CFAR thresholds image, detected frequency components and frame (time) fusion results.

5.3.1 "Ferry" Boat Signal Multiple Frame Detection and Fusion Test

The proposed Median CFAR and multi-frame fusion algorithm has been tested on "Ferry" boat signal, and the test results of the 'Ferry' test case with multiple frame detection and fusion are shown in Fig. 12.

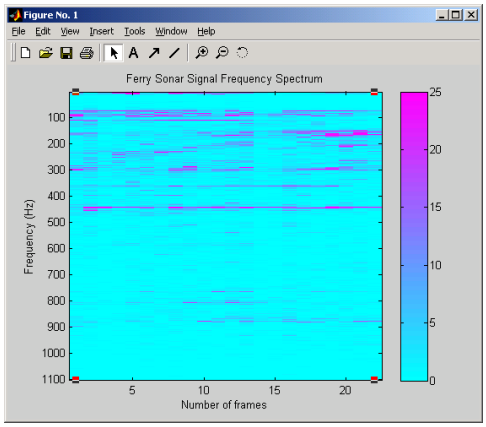

(a) 'Ferry' boat signal spectrum over multiple frames

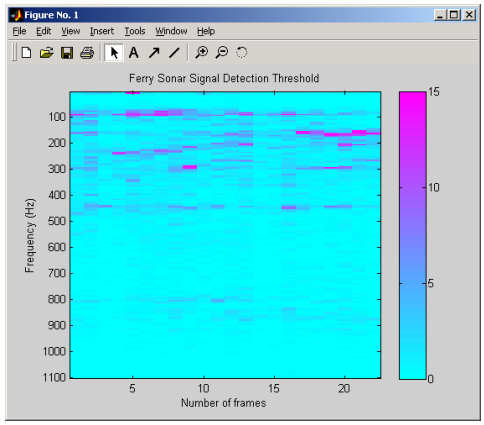

(b) 'Ferry' signal spectrum threshold image calculated by proposed Median CFAR algorithm with window size of 5

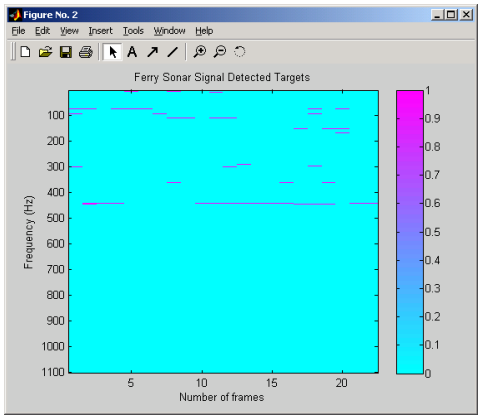

(c) Detected target frequency components by using the proposed Median CFAR algorithm with window size of 5 and default sensitivity

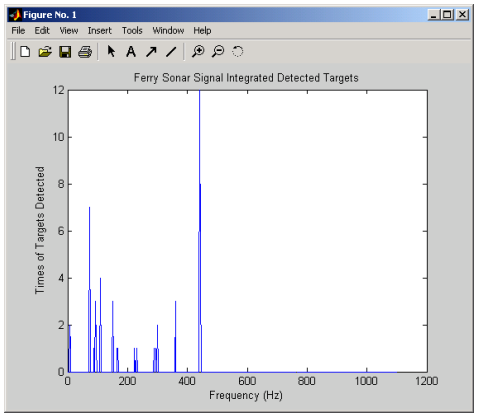

(d) Integrated detected target frequency components with frames (time)

FIGURE 12: Multiple frame frequency components detection and fusion results ("Ferry" signal by using the proposed adaptive CFAR algorithm with window size of 5).

Fig. 12 (a) shows us that the "Ferry" boat signal has a pretty wide frequency band, which spreads between about 60 to 450 Hz, with the main frequency component at about 440 Hz, and the strength of these frequency components are between 10 to 25 dB. Fig. 12 (b) shows us the Median CFAR threshold image of Fig. 12 (a), in which we can see that the higher the background noise, the higher the threshold, and threshold image strength values are between 5 to 15 dB. Fig. 12 (c) shows us the detected target frequency components by using the proposed Median CFAR Algorithm, in which we can see that the main frequency around 440 Hz has been successfully detected. Some other frequency components between 60 to 450 Hz are also successfully detected. Fig. 12 (d) shows us the integrated detected target frequency components of Fig. 12 (c), in which we can see that the detection rates of the two biggest frequency components (around 440 and 70 Hz) are 55% (12/22) and 32% (7/22), and these two main frequency components are finally successfully detected by vector (distribution) normalization and final thresholding, and their detected frequencies are 71.06 Hz and 439.28 Hz. Fig. 12 (d), also shows us that there are some frequency components between 60 and 450 Hz, in which their detection rates are relatively lower, and they did not cross the final threshold after distribution normalization.

5.3.2 "Naiad1" Boat Signal Multiple Frame Detection and Fusion Test

The proposed Median CFAR and multi-frame fusion algorithm has also been tested on "Naiad1" boat signal. The test results of the 'Naiad1' test case with multiple frame detection and fusion are shown in the Fig. 13.

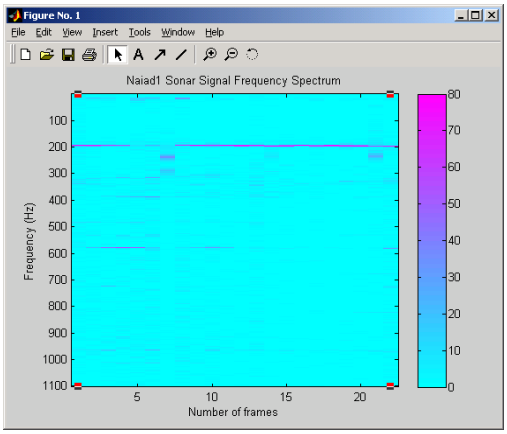

(a) 'Naiad1' signal spectrum over multiple frames

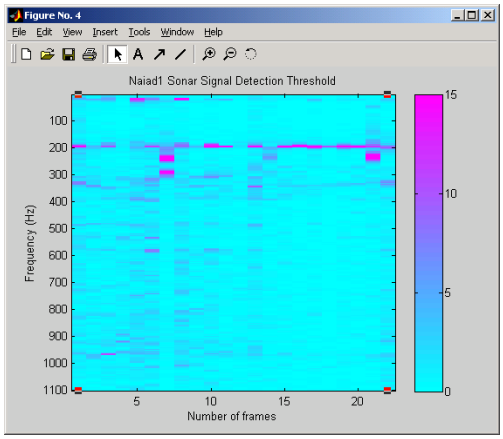

(b) 'Naiad1' signal spectrum threshold image calculated by the proposed Median CFAR algorithm with window size of 5.

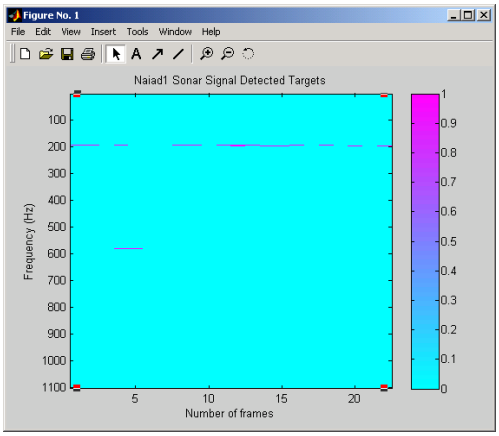

(c) Detected target frequency components by using the proposed Median CFAR algorithm with window size of 5 and default sensitivity.

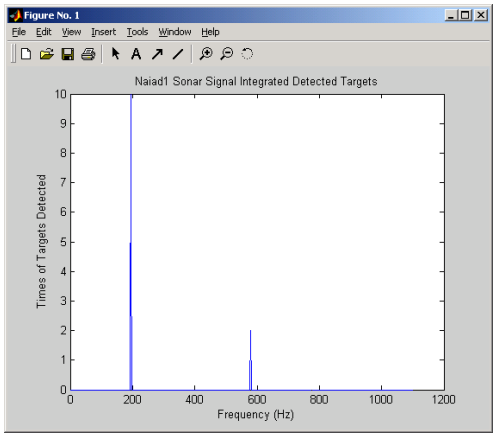

(d) Integrated detected target frequency components by using the proposed Median CFAR algorithm with window size of 5 and default

FIGURE 13: Multiple frame target frequency detection and fusion results of 'Naiad1' by using the proposed Median CFAR algorithm with window size of 5.

Fig. 13 (a) shows us that the 'Naiad1' boat signal has a pretty narrow frequency band, mainly located around 190 Hz, with some small pieces around 580 Hz, and the strength of these frequency components are between 30 to 70 dB. Fig. 13 (b) shows us the Median CFAR threshold image of Fig. 13 (a), in which we can see that the threshold image strength values are between 5 to 15 dB. Fig. 13 (c) shows us that the detected target frequency components by using Median CFAR Algorithm, in which we can see that the main frequency component around 190 Hz has been successfully detected, and a few other frequency components around 580 Hz are also successfully detected. Fig. 13 (d) shows us the integrated detected target frequency components of Fig. 13 (c), in which we can see that the detection rates of the biggest frequency component (around 190 Hz) is 46% (10/22), and the main frequency component is finally successfully detected by vector (distribution) normalization and final thresholding, and its detected frequency is 191.65 Hz. In Fig. 13 (d), we can also see that there is a frequency component around 580 Hz,

in which the detection rate is relatively lower and it did not cross the final threshold after distribution normalization.

5.3.3 'Naiad2' Boat Signal Multiple Frame Detection Test

The proposed Median CFAR and multi-frame fusion algorithm has been tested on 'Naiad2' boat signal, and the test results of the 'Naiad2' test case with multiple frame detection and fusion are shown in Fig. 14.

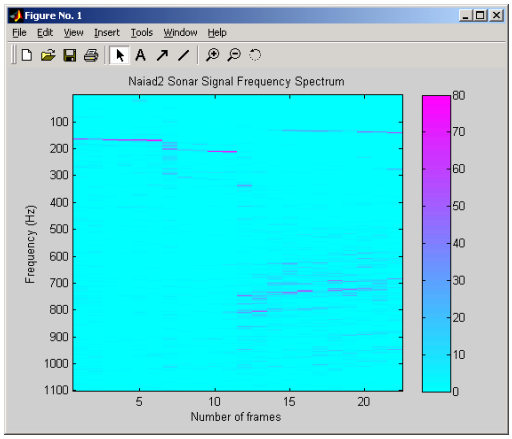

(a) 'Naiad2' boat signal spectrum over multiple frames

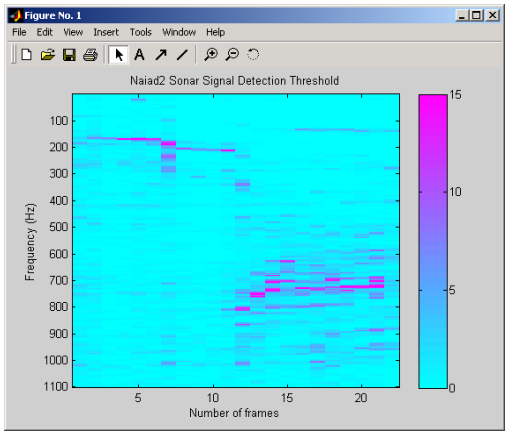

(b) 'Naiad2' signal spectrum threshold image calculated by using the proposed Median CFAR algorithm with window size of 5

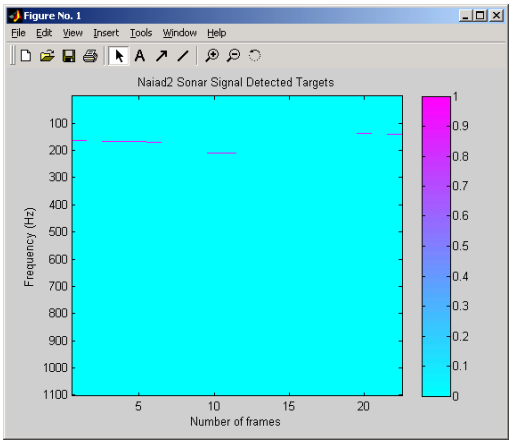

(c) Detected target frequency components by using the proposed Median CFAR algorithm with window size of 5 and default sensitivity

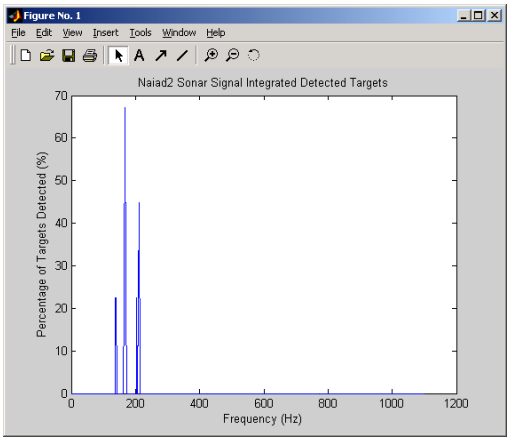

(d) Integrated detected target frequency components by using the proposed Median CFAR algorithm with window size of 5 and default sensitivity

FIGURE 14: Multiple frame target frequency detection and fusion results of 'Naiad2' by using the proposed Median CFAR Algorithm with window size of 5.

Fig. 14 (a) shows us that the 'Naiad2' boat signal has a diverse frequency distribution, and the main boat generated frequency components are around 170 Hz with some frequency increasing and decreasing (probably due to the accelerating or slowing down of the boat), and the strength of these frequency components are between 30 to 70 dB. There is also some clutter (noise) spread between 500 to 1000 Hz, which are definitely not boat-generated frequency components. Fig. 14 (b) shows us the threshold image of Fig. 14 (a) that is calculated by the proposed adaptive Median CFAR algorithm, in which we can see that the threshold image strength values are between 5 to 15 dB (which are much smaller than the maximum value of signal components of 80 dB). We can also see that the thresholds around the unknown clutter noise area between

500 to 1000 Hz are very strong (about 15 dB), which are very helpful at removal of possible false detection. Fig. 14 (c) shows us the detected target frequency components by using Median CFAR Algorithm, in which we can see that the main frequency around 170 Hz has been successfully detected, and the false detection possibly caused by some other unknown clutter (noise) frequency components between 500 to 1000 Hz are successfully avoided (The clutter will probably cause false detection, if we use constant threshold that is normally used in acoustic signal processing and detection.). Fig. 14 (d) shows us the integrated detected target frequency components of Fig. 14 (c), in which we can see that the detection rates of the three biggest frequency components (around 170 Hz) are 68% (about 165 Hz), 45% (around 210 Hz) and 23% (around 130 Hz), and the biggest main frequency component was finally successfully detected by vector (distribution) normalization and final thresholding, and its detected frequency is 165.81 Hz. In Fig. 12 (d), we can also see that the second and third biggest frequency components did not cross the final threshold (under the 50% final detection threshold) after distribution normalization.

5.3.4 'Reef Heron1' Boat Signal Multiple Frame Detection and Fusion Test

The proposed Median CFAR and multi-frame fusion algorithm has been tested on 'Reef Heron1' boat signal, and the test results of the 'Reef Heron1' test case with multiple frame detection and fusion are shown in Fig. 15.

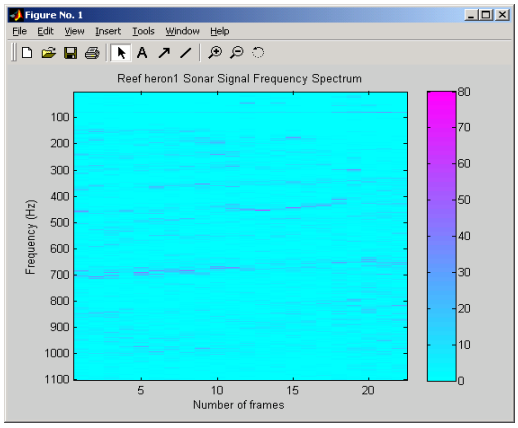

(a) 'Reef Heron1' boat signal spectrum over multiple frames

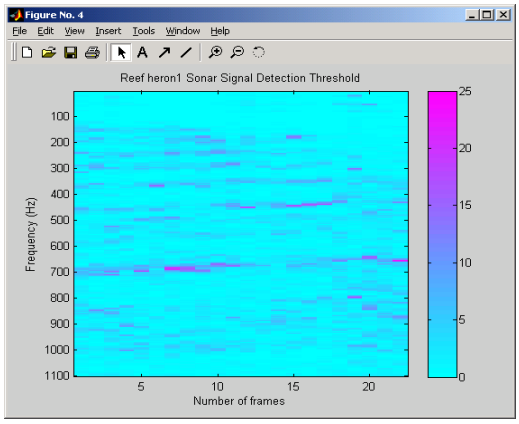

(b) 'Reef Heron1' boat signal spectrum threshold image calculated by the proposed Median CFAR algorithm with window size of 5

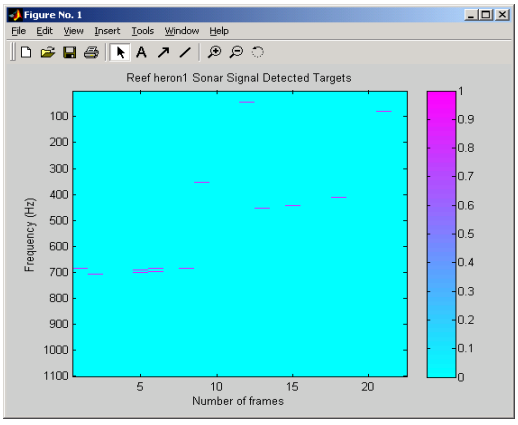

(c) Detected target frequency components by using the proposed Median CFAR algorithm with the window size of 5 and default sensitivity

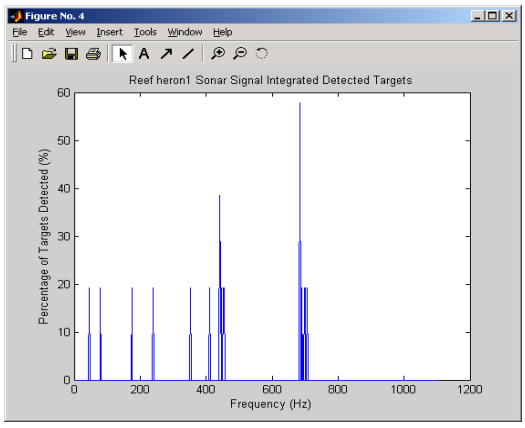

(d) Integrated detected target frequency components by using the proposed Median CFAR algorithm with the window size of 5 and default sensitivity

FIGURE 15: Multiple frame target frequency detection and fusion results of 'Reef heron1' by using the proposed Median CFAR algorithm with window size of 5

Fig. 15 (a) shows us that the “Reef Heron1” boat signal has pretty loosely distributed frequency components in a very broad band range (in terms of our observation range), which spreads from about 10 to 1000 Hz, with the strongest frequency components are around 680 and 450 Hz, and the strength of these frequency components are between 30 to 45 dB. Fig. 15 (b) shows us the Median CFAR threshold image of Fig. 15 (a), in which we can see that the threshold image strength values are between 10 to 20 dB. Fig. 15 (c) shows us the detected target frequency components by using Median CFAR Algorithm, in which we can see that the two main frequency components at around 680 and 450 Hz have been successfully detected, and some other frequency components between 10 to 450 Hz are also crossed the Median CFAR thresholds. Fig. 15 (d) shows us the integrated detected target frequency components of Fig. 15 (c), in which we can see that the detection rates of the biggest frequency component (around 680 Hz) is 58%, and this main frequency component was finally successfully detected by vector (distribution) normalization and final thresholding, and its detected frequency is 682.60 Hz. In Fig. 15 (d), we can also see that there are some frequency components between 10 and 450 Hz, in which the detection rates are relatively lower, and that did not cross the final threshold after distribution normalization.

5.3.4 ‘Reef Heron2’ boat signal multiple frame detection and fusion test

The proposed Median CFAR and multi-frame fusion algorithm has been tested on “Reef Heron2’” boat signal, and the test results the ‘Reef Heron2’ test case with multiple frame detection and fusion are shown in Fig. 16.

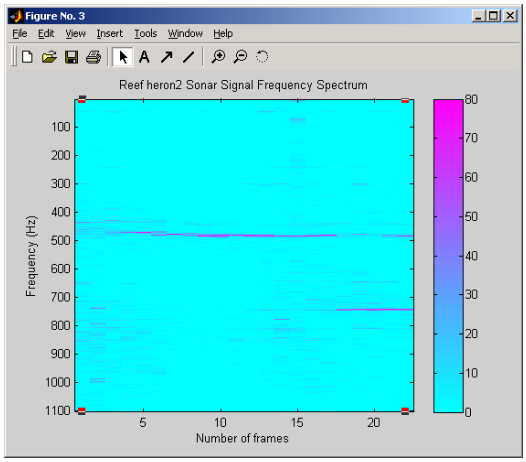

(a) ‘Reef Heron2’ boat signal spectrum over multiple frames

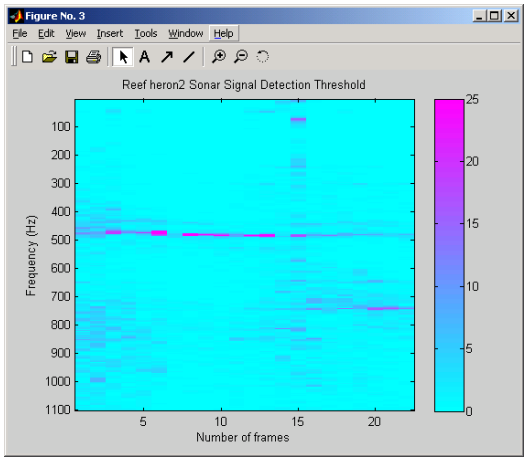

(b) ‘Reef Heron2’ boat signal spectrum threshold image calculated by the proposed Median CFAR algorithm with the window size of 5

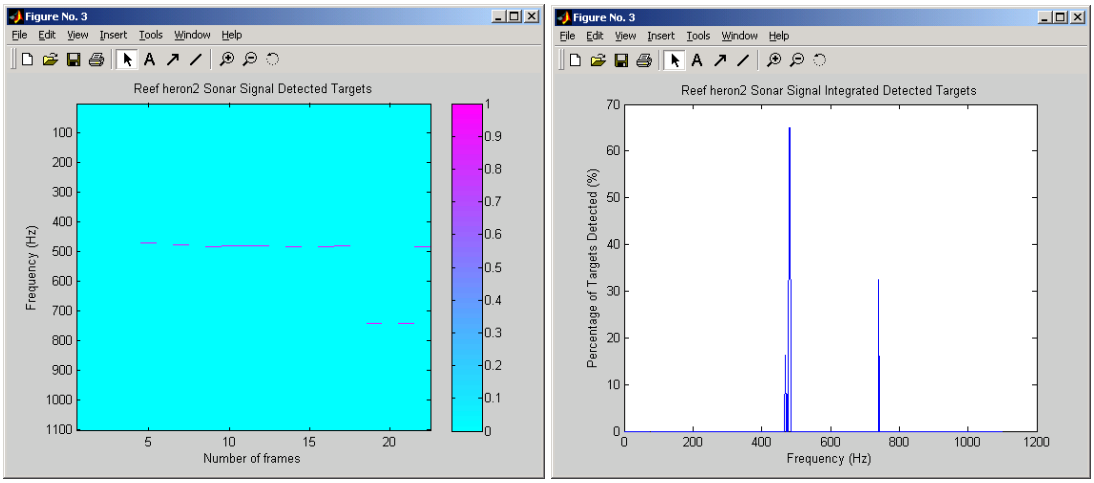

(c) Detected target frequency components by using the proposed Median CFAR algorithm with window size of 5 and a default sensitivity

(d) Integrated detected target frequency components by using the proposed Median CFAR algorithm with window size of 5 and a default sensitivity.

FIGURE 16: Multiple frame target frequency components detection and fusion results ("Reef Heron2" by using the proposed Median CFAR algorithm with window size of 5).

Fig. 16 (a) shows us that there are two main frequency components around 480 and 740 Hz in the 'Reef Heron2' boat signal, and there are some frequency shifts around 480 Hz, probably because of the change of the speed of boat engine. And there are some unknown clutter frequency components that are around 800 Hz with the strength between 30 to 50 dB. Fig. 16 (b) shows us that Median CFAR threshold image of Fig. 16 (a), in which we can see that the threshold image strength values are between 10 to 25 dB. Fig. 16 (c) shows us that the detected target frequency components by using Median CFAR Algorithm, in which we can see that the two main frequency components at around 480 and 740 Hz have been successfully detected, but some other sea clutter frequency components are too low to cross the Median CFAR thresholds, in which some false detection are avoided. Fig. 16 (d) shows us the integrated detected target frequency components of Fig. 16 (c), which shows us that there are several frequency components around 700 Hz, and the detection rate of the biggest one around 680 Hz is above 65%. And the main frequency components that were successfully detected finally by vector (distribution) normalization and final thresholding, are 478Hz and 480Hz. In Fig. 16 (d), we can also see that the second biggest frequency component around 740 Hz, for which it's the detection rate is relatively lower, did not cross the final threshold after distribution normalization (under the 50% final detection threshold).

5.3.5 'Kuala Lumpur' Boat Signal Multiple Frame Test

The proposed Median CFAR and Multi-Frame Fusion Algorithm has been tested on "Kuala Lumpur" boat signal, and the test results of the 'Kuala Lumpur' test case with multiple frame detection and fusion are shown in Fig. 17.

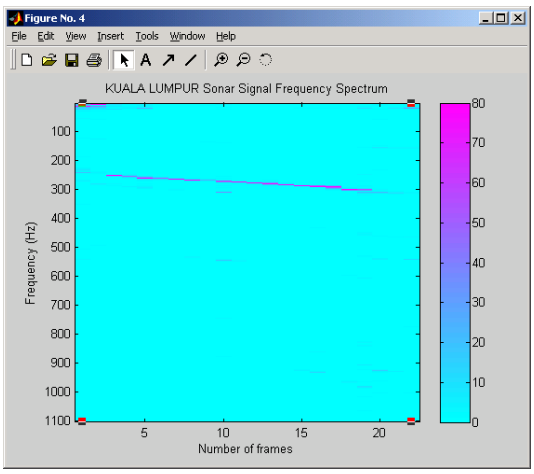

(a) 'Kuala Lumpur' boat signal spectrum over multiple frames

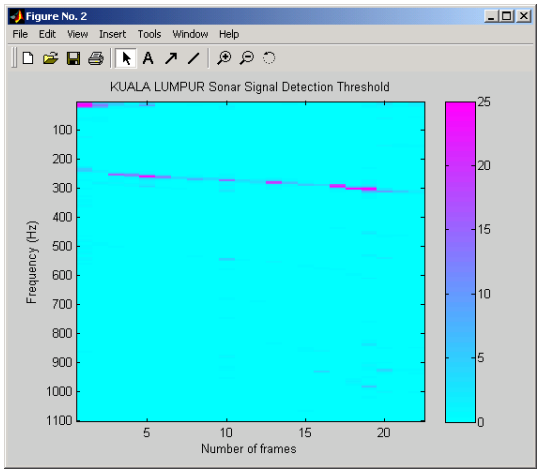

(b) 'Kuala Lumpur' boat signal spectrum threshold image calculated by the proposed Median CFAR algorithm with the window Size of 5

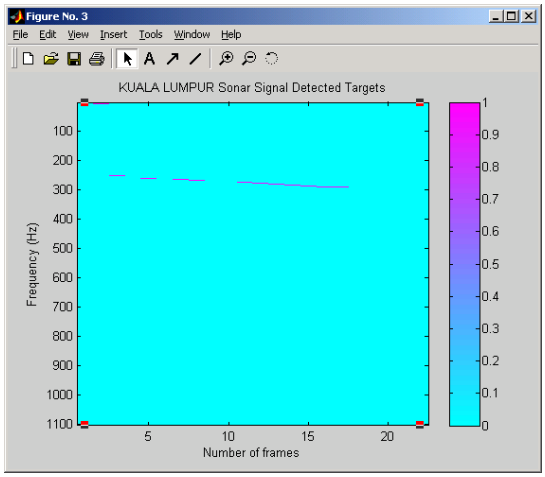

(c) Detected target frequency components using the proposed Median CFAR algorithm with the window size of 5 and a default sensitivity

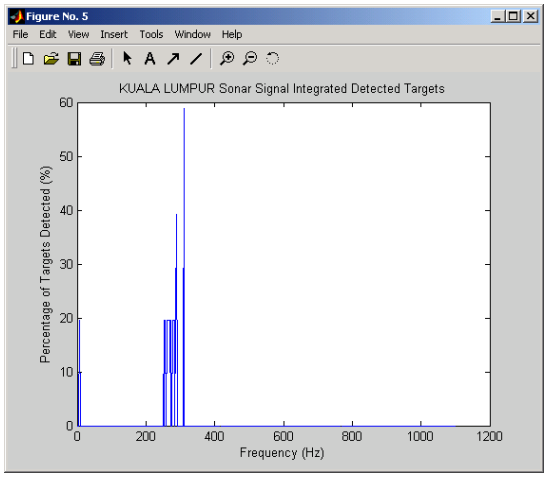

(d) Integrated detected target frequency components by using the proposed Median CFAR algorithm with the window Size of 5 and a default sensitivity

FIGURE 17: Multiple frame target frequency detection fusion results of 'Kuala Lumpur' by using the proposed Median CFAR algorithm with the window size of 5

Fig. 17 (a) shows us that the 'Kuala Lumpur' boat signal has one clear main frequency strip (components) which are located around 310 (around 310 Hz, there is some frequency quick increase in a very short time, probably because the speed of boat engine was increasing), and the strength of these frequency components are between 30 to 50 dB. Fig. 17 (b) shows us the Median CFAR threshold image of Fig. 16 (a), in which we can see that the threshold image strength values are between 5 to 25 dB. Fig. 17 (c) shows us the detected target frequency components by using Median CFAR Algorithm, in which we can see that the main frequency component at around 280Hz have been successfully detected, and some other frequency components a little below 280 Hz are also successfully detected. Fig. 17 (d) shows us the integrated detected target frequency components of Fig. 17 (c), in which we can see the detection rates of the biggest frequency component (around 680 Hz) is 65%, and this main frequency component was finally successfully detected by vector (distribution) normalization and final thresholding, and its detected frequency is 307.93Hz. In Fig. 17 (d), we can also see some other frequency components just below 307.93 Hz, in which the detection rates are relatively lower, and did not cross the final threshold after distribution normalization (under the 50% final detection threshold).

5.3.6 'No signal' with only 'white Gaussian noise' test - multiple frame test results

The proposed Median CFAR and multi-frame fusion algorithm has been tested with 'No Signal' but only 'White Gaussian Noise' situation and the test results of the 'White Gaussian Noise' test case with multiple frame detection and fusion are shown in Fig. 18.

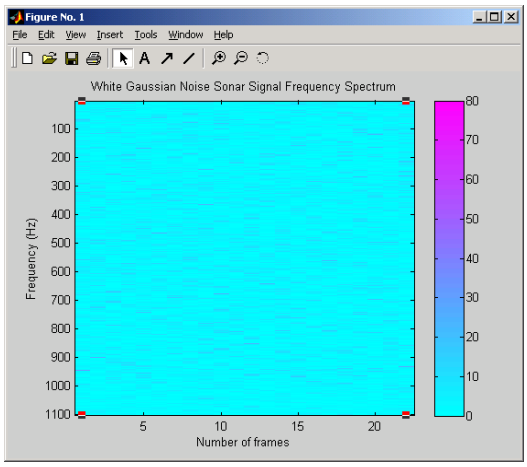

(a) 'White Gaussian Noise' signal spectrum over multiple frames

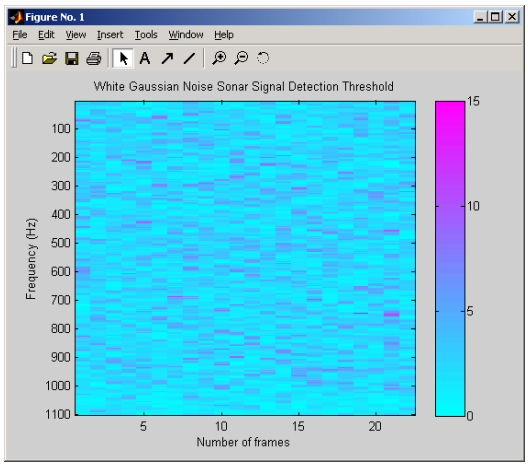

(b) 'White Gaussian Noise' signal spectrum threshold Image calculated by the proposed Median CFAR algorithm with the window size of 5

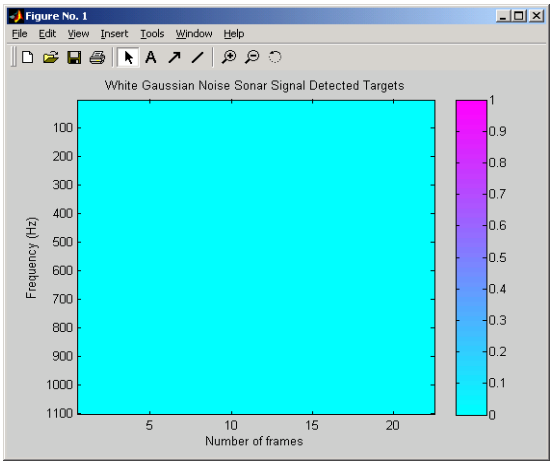

(c) Detected target frequencies using the proposed Median CFAR algorithm with the window size of 5 and a default sensitivity

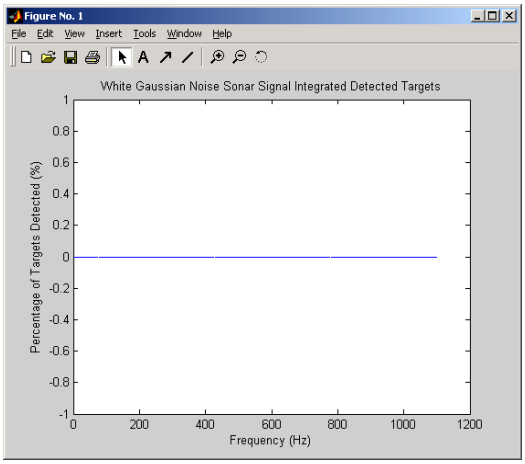

(d) Integrated detected target frequencies using the proposed Median CFAR algorithm with the window size of 5 and a default sensitivity

FIGURE 18: Multiple frame target detection fusion results of no signal but only gaussian noise

Fig. 18 shows us that no target is detected and proved that the proposed Median CFAR and Multi-Frame Fusion Algorithm can deal with the 'No Signal' case very well, which is often the case in a very quiet ocean area with no boat traffic. This is due to the fact that the CFAR algorithm is based on the idea of comparison of each frequency bin pixel with its neighborhood background noise. In this test case, the difference between the value of every frequency bin pixel bin and their thresholds is too small to cross the detection threshold.

6. RELATED WORKS AND DISCUSSION

In this paper, a novel Adaptive Constant False Alarm Rate (ACFAR) and Post Detection Fusion algorithms have been proposed for an effective automatic detection of marine vehicle generated acoustic signal spectrum signature.

1. Compared with the traditional average CFAR algorithm (CA CFAR and CAGO CFAR) [23], the proposed Median CFAR algorithm has the ability to remove the effects of signal components while estimating the background noise, so the estimated noise level is much more accurate, especially when there is signal component in certain frequency bin.
2. Compared with some other ship signature measurement algorithms, such as Kil Woo Chung etc. DEMON Acoustic Ship Signature Measurements [34], the proposed detection algorithm has extremely low false alarm (almost never has any false alarm), because of the accurate estimate the background noise.
3. Compared with Hamed Komari Alaie and Hassan Farsi's statistical algorithm [35], the proposed algorithm is much easier for future engineering application.

7. CONCLUSIONS AND FUTURE WORK

In this paper, an Adaptive Constant False Alarm Rate (ACFAR) and post detection fusion algorithms have been proposed based on the Neyman-Pearson criterion for an effective automatic detection of marine vehicle generated acoustic signal spectrum signature, in which a low constant false alarm rate is kept with extremely high detection rate. The proposed algorithms have been tested on real acoustic signals recorded from hydrophone, called 'Kimbla', 'Ferry', 'Naiad1', 'Naiad2', 'Reef heron1', 'Reef heron2' and 'Kuala Lumpur' marine vehicle signals and also on a pattern of white noise. The statistical analysis and experimental results showed that the proposed algorithm has kept a very low false alarm rate and extremely high detection rate.
The following conclusions can also be drawn:

1) The proposed adaptive CFAR algorithm is used to detect signal spectrum signature in single frame, which will keep our automatic target detection system at lower and constant false alarm rate. This algorithm is especially good for detecting LOFAR target frequency components.
2) The bigger the Median CFAR window, the lower frequency components in the threshold signal image. In our experiment, the Median CFAR window size of 5 is appropriate for most cases.
3) A magnitude (in the frequency domain) normalization and 40 dB amplification are used to keep our automatic detector more robust.
4) With the default sensitivity value, most marine vehicle generated signal frequency components are correctly detected. Decreasing sensitivity value makes the false detection rate (alarm rate) lower, and less frequency components will be detected at the same time.
5) The fusion of single frame detected frequency components will make the detection much more robust. For example, with the fusion of 20 frames, the possibility of correct target detection increases dramatically.
6) In order to deal with various kinds of detected targets situation and increase the probability of target detection, 'Integrated targets vector normalization ($k_p \, p/\|p\|$)' and 40 dB amplification are used to keep our final detection more robust and reliable (increase probability of correct detection.).
7) In the experiments, the detected boat generated frequencies of 'Kimbla', 'Ferry', 'Naiad1', 'Naiad2', 'Reef heron1', 'Reef heron2' and 'Kuala Lumpur' are 159.35 Hz, 71.06 Hz (and 439.28 Hz), 191.65 Hz, 165.81 Hz, 682.6025 Hz, 478.0371Hz (and 480.1904) Hz, and 307.9248 Hz respectively, which correspond very closely to the "ground truth".
8) In the 'No Signal' with only 'White Gaussian Noise' test case, no target frequency component is detected. That proved that the proposed Median CFAR and Multi-Frame Fusion Algorithm can deal with 'No Signal' case very well. That because of the CFAR algorithm is based on the idea of comparison of each frequency bin pixel with its neighborhood background noise. In this test case, the difference between the value of every frequency bin pixel bin and their thresholds is too small to cross 'the detection threshold'.

Future work:

1) Recognition - The detected spectrum signatures can be used for ship recognition and tracking in the future, in which the study of similarity measures between ship spectrum

signatures, and the neural network can also be possibly applied for the recognition of detected ships, based on a database of collected spectrum signatures.

2) Tracking-The proposed real time processing and detecting based sonars can be connected into a worldwide undersea network, in which the ships around each sonar can be detected, tracked, and displayed in a control center.
3) Arrays processing - Sonar array processing based on the proposed algorithm as a building block can also be used to increase the SNR of input signal, or detect the direction of incoming ships,

8. ACKNOWLEDGMENT

The research is supported by 2017 Changshu Scientific and Technology Development Plan Project (CQ201701), and the test data was provided by Sonarcom PTY LTD in Australia.

9. REFERENCES

[1] S. Lawrence Marple Jr., "Digital Spectral Analysis with Applications". Prentice Hall, Inc., 1987.

[2] Chan, Y. T., "Underwater Acoustic Data Processing", NATO ASI Series, Kluwer Academic Publishers.

[3] A. D. Waite, "Sonar for Practising Engineers", John Willey & Sons, LTD.

[4] Urick, R. J. (1983). Principles of Underwater Sound. New York, McGraw-Hill Book Company.

[5] Lurton, X. (2002). An Introduction to Underwater Acoustics: Principles and Applications. Chichester, UK, Springer/Praxis.

[6] Etter, P. C. (1992). Underwater Acoustic Modeling: Principles, Techniques and Applications. New York, Elsevier.

[7] Burdic, W. S., 1984, "Underwater Acoustic System Analysis", Prentice-Hall, Englewood Clissf, NJ.

[8] J. X. Qiu, L. Zheng, Y. C. Wang, "Research on ship-radiated noise beat tune", Technical Acoustics, vol. 33, no. 4, pp. 322-325, 2014.

[9] F. S. Zhang, D. Feng, "Fusion and extraction of modulation feature from ship radiated-noise based on wavelet packet and ZFFT", Electronics World, vol. 14, no. 2, pp. 105-106, 2014.

[10] X. W. Luo, S. L. Fang, "Feature extraction from non-stationary amplitude modulated broad-band signal using the Hilbert-Huang transform", Signal Processing, vol. 27, no. 6, pp. 950-955, 2011.

[11] Xueyao Li; Fuping Zhu; Harbin Eng. and Harbin University, Application of the zero-crossing rate, LOFAR spectrum and wavelet to the feature extraction of passive sonar signals, Proceedings of the 3rd World Congress on Intelligent Control and Automation, 2000., vol.4, pp. 2461-2463 (2000).

[12] G. Q. Wu, "Ship radiated-noise recognition (I) the overall framework analysis and extraction of line-spectrum", Acta Acoustica, vol. 23, no. 5, pp. 394-400, 1998.

[13] Y. S. Cheng, X. Gao, H. Liu, "A method for ship propeller blade-number recognition based on template matching", TechnicaI Acoustic, vol. 29, no. 2, pp. 228-231, 2010.

[14] Peng H.C., Long F., and Ding C., Feature selection based on mutual information: criteria of max-dependency, max-relevance, and min-redundancy, IEEE Transactions on Pattern Analysis and Machine Intelligence, Vol. 27, No. 8, pp. 1226-1238 (2005).

[15] Roholing, H., "Radar CFAR Thresholding in Clutter and Multiple Target Situations", IEEE Transactions on Aerospace and Electronic System, Vol. AES-19, No. 4, July 1983, pp. 608-621.

[16] Merrill I, Skolnik, "Introduction to Radar Systems". McGraw-Hill Book Company, 1980.

[17] S. Wang, J. X. Qiu, S. J. Wang, "Enhancement of ship radiated noise DEMON spectrum SNR based on correlation properties theory of principles of system_dynamics", Ship Science and Technology, vol. 35, no. 8, pp. 24-27, 2013.

[18] Y. S. Cheng, Y. C. Wang, "DEMON analysis of underwater target radiation noise based on modern signal processing", Technical Acoustics, vol. 25, no. 1, pp. 71-74, 2006.

[19] Eric Dahai Cheng, Subhash Challa, Xuanchen Tang and Xiaohu Liu, "Non-Cooperative Object Detection in Sea Using Acoustic Sensors" accepted by the Digital Image Computing: Techniques and Applications, 1-3 December 2010, Sydney, Australia. (DICTA 2010), pp294-310.

[20] Eric Dahai Cheng, Massimo Piccardi and Tony Jan, "Boat-Generated Acoustic Target Signal Detection by Use Of An Adaptive Median CFAR and Multi-Frame Integration Algorithm", The 2005 European Signal Processing Conference (EUSIPCO-2005), September 4-8, Antalya, Turkey.

[21] Eric D. Cheng, Massimo Piccardi and Tony Jan, "Stochastic Boat-Generated Acoustic Target Signal Detection in Time-Frequency Domain" IEEE International Symposium on Signal Processing and Information Technology (ISSPIT'04), Rome, Italy, December, 2004.

[22] Vera P. Behar, "Adaptive CFAR PI Processor for Radar Target Detection in Pulse Jamming", Journal of VLSI Signal Processing Vol. 26, pp. 383-396, 2000.

[23] Levanon, N., Shor, M., "Order Statistic CFAR for Weibull Background", IEE Proceeding, Vol. 137, No. 3, June 1990, pp. 157-162.

[24] Roholing, H., "Radar CFAR Thresholding in Clutter and Multiple Target Situations", IEEE Transactions on Aerospace and Electronic System, Vol. AES-19, No. 4, July 1983, pp. 608-621.

[25] I.G. Prokopenko, F.J. Yanovsky, L.P. Ligthart, "Adaptive Algorithms for Weather Radar", Proceedings of the European Radar Conference (EuRAD 2004), pp. 329-332, 2004.

[26] A. D. Whalen, "Detection of Signals in Noise". New York, Academic, 1971, pp. 231-235.

[27] H. L.Van Trees, "Detection, Estimation and Modulation Theory". Part I. New York, Wily, 1968, pp. 68-85.

[28] Henry Stark, John W. Woods, "Probability and random process with applications to signal processing", Prentice Hall, 3rd edition, 2001.

[29] M. D. Srinach, P. K. Rajasekaran and R. Viswanathan, "Introduction to statistical signal processing with applications", Prentice Hall, Englewood Cliff, New Jersey.

[30] R. Cucchiara, C. Grana, M. Piccardi, and A. Prati, "Statistic and Knowledge-baseeticd Moving Object Detection in Traffic Scenes", in Proc. of ITSC-2000 - The 3rd Annual IEEE Conference on Intelligent Transportation Systems, Oct. 1-5, 2000, Dearborn, MI, USA, pp. 27-32.

[31] Charles W. Therrien, "Discrete Random Signals and Statistical Signal Processing", Prentice Hall, Englewood Cliffs, NJ 07632.

[32] H. M. Finn and R. S. Johnson, "Adaptive Detection Mode with Threshold Control as a Function of Spatially Sampled Clutter Level Estimates", RCA Review, Vol. 29, No. 3, pp. 414, September 1968.

[33] Ritcey, J. A., "Performance Analysis of the Censored Mean-Level Detector", IEEE Transactions on Aerospace and Electronic System, Vol. AES-22, No. 6, July 1986, pp. 443-453.

[34] Advances in Acoustics and Vibration, Volume 2011 (2011), Article ID 952798, 13 pages, http://dx.doi.org/10.1155/2011/952798.

[35] Hamed Komari Alaie, and Hassan Farsi, "Passive Sonar Target Detection Using Statistical Classifier and Adaptive Threshold", Appl. Sci. 2018, 8(1), 61; doi:10.3390/app8010061.

[36] David C. Swanson, "Signal Processing for Intelligent Sensor Systems", Marcel Dekker. Inc.

[37] Richard O. Nielsen, "Sonar Signal Processing", Artech House.

[38] Nielson, R. O. (1991). Sonar Signal Processing. Norwood, MA, Artech House.

[39] Robinson, A. R. and D. Lee, Eds. (1994). Oceanography and Acoustics Prediction and Propagation Models. Modern Acoustics and Signal Processing. Woodbury, NY, AIP Press.

[40] R. O. Nielsen, "Sonar Signal Analysis". Boston, MA, Artech House, 1991, pp. 123-128.

[41] Stergios Stergiopoulos, "Advanced Signal Processing Handbook", CRC Press.

[42] Todd K. Moon and Wynn C. Stirling, "Mathematical Methods and Algorithms for Signal Processing", Prentice-Hall,Upper Saddle River, NJ 07458.